Article

AGS3 and Gα$_{i3}$ Are Concomitantly Upregulated as Part of the Spindle Orientation Complex during Differentiation of Human Neural Progenitor Cells

Jackson L. K. Yip [1,†]**, Maggie M. K. Lee** [1]**, Crystal C. Y. Leung** [1]**, Man K. Tse** [1]**,**
Annie S. T. Cheung [1] **and Yung H. Wong** [1,2,*]

[1]   Division of Life Science and the Biotechnology Research Institute, Hong Kong University of Science and
     Technology, Clear Water Bay, Kowloon, Hong Kong 999077, China; lkyip@connect.ust.hk (J.L.K.Y.);
     mgleebiochem@yahoo.com.hk (M.M.K.L.); crystal.cyleung@gmail.com (C.C.Y.L.);
     mk.jack.tse@gmail.com (M.K.T.); anniecst@ust.hk (A.S.T.C.)
[2]   State Key Laboratory of Molecular Neuroscience, Hong Kong University of Science and Technology,
     Clear Water Bay, Kowloon, Hong Kong 999077, China
[*]   Correspondence: boyung@ust.hk; Tel.: +852-2358-7328; Fax: +852-2358-1552
[†]   Present address: School of Health and Biomedical Sciences, RMIT University, PO Box 71, Bundoora,
     Victoria 3083, Australia.

check for
updates

Abstract: Adult neurogenesis is modulated by many G$_i$-coupled receptors but the precise mechanism remains elusive. A key step for maintaining the population of neural stem cells in the adult is asymmetric cell division (ACD), a process which entails the formation of two evolutionarily conserved protein complexes that establish the cell polarity and spindle orientation. Since ACD is extremely difficult to monitor in stratified tissues such as the vertebrate brain, we employed human neural progenitor cell lines to examine the regulation of the polarity and spindle orientation complexes during neuronal differentiation. Several components of the spindle orientation complex, but not those of the polarity complex, were upregulated upon differentiation of ENStem-A and ReNcell VM neural progenitor cells. Increased expression of nuclear mitotic apparatus (NuMA), Gα$_i$ subunit, and activators of G protein signaling (AGS3 and LGN) coincided with the appearance of a neuronal marker (β-III tubulin) and the concomitant loss of neural progenitor cell markers (nestin and Sox-2). Co-immunoprecipitation assays demonstrated that both Gα$_{i3}$ and NuMA were associated with AGS3 in differentiated ENStem-A cells. Interestingly, AGS3 appeared to preferentially interact with Gα$_{i3}$ in ENStem-A cells, and this specificity for Gα$_{i3}$ was recapitulated in co-immunoprecipitation experiments using HEK293 cells transiently overexpressing GST-tagged AGS3 and different Gα$_i$ subunits. Moreover, the binding of Gα$_{i3}$ to AGS3 was suppressed by GTPγS and pertussis toxin. Disruption of AGS3/Gα$_{i3}$ interaction by pertussis toxin indicates that AGS3 may recognize the same site on the Gα subunit as G protein-coupled receptors. Regulatory mechanisms controlling the formation of spindle orientation complex may provide novel means to manipulate ACD which in turn may have an impact on neurogenesis.

Keywords: AGS3; G protein; LGN; neurogenesis; NuMA; Ric-8A

1. Introduction

Neurogenesis is a highly regulated process by which new neurons are spawned from neural stem cells and progenitor cells, and it is absolutely essential for the development of the brain and our nervous system [1]. In adulthood, functional neurons can still be generated from specific brain

regions such as the subgranular zone of the hippocampus. Manipulation of adult neurogenesis to generate new neurons may thus hold the key to curative therapy against neurodegenerative diseases. However, the molecular mechanism by which neural stem cells become mature neurons is not well understood. Because the population of neural stem cells is limited, it is critical for these specialized cells to maintain their own population while giving rise to new neurons. This is achieved by asymmetric cell division (ACD), a process through which the neural stem cell can achieve self-renewal in one of the two daughter cells, as well as differentiating into different corresponding progenitors and eventually into various neuronal types such as glial cells, oligodendrocytes and mature neurons [2,3]. Hence a thorough understanding of the initiation and regulation of ACD may offer the opportunity to manipulate neurogenesis for therapeutic purposes.

ACD is mainly regulated by two protein complexes that are evolutionarily conserved. They are the polarity complex which is made up of partition defective 6 (Par6), Par3 and atypical protein kinase C (aPKC) [4], and the spindle orientation complex composed of nuclear mitotic apparatus (NuMA), activator of G protein signaling (AGS) and $G\alpha_i$ subunit [5]. The Par6/Par3/aPKC tripartite complex is conserved from worms to vertebrates and is responsible for establishing apical–basal polarity. Par3 is thought to provide anchorage to assemble the polarity complex at the apical–lateral border by binding Par6 and recruiting Par6-associated proteins including aPKC. In mammalian cells, spindle positioning is achieved by the binding of the spindle orientation complex to the polarity complex through the ankyrin protein inscuteable (mInsc) [6,7]. It is generally believed that the binding of $G\alpha_i$ to an AGS protein (e.g., AGS3 and AGS5/LGN) increases the latter's affinity for NuMA which, in turn, interacts with dynein and exert forces to orient the spindle [8–10]. These mechanistic insights were initially derived from invertebrate model systems (*Drosophila* and *C. elegans*) and they are difficult to validate in complex stratified vertebrate systems where the outcome of neural progenitor/stem cell division varies [3]. Moreover, the signals that trigger the assembly of the polarity and spindle orientation complexes and the fate of the individual components remain largely unknown. A thorough understanding of how these proteins are regulated is especially important in adult neurogenesis, because neural stem cells do not undergo ACD spontaneously. The involvement of $G\alpha_i$ and AGS proteins in the spindle orientation complex adds another level of complexity to ACD since many G protein-coupled receptors (GPCRs) can modulate adult neurogenesis [11] while AGS proteins also participate in other neuronal functions such as drug addiction that involve G_i-coupled receptors [12].

Since both polarity and spindle orientation complexes participate in ACD, monitoring their regulation during the differentiation of neural progenitor stem cells may provide clues to decipher the signals that initiate ACD. However, it remains highly challenging to quantitatively measure the functions of neural progenitor stem cells and their differentiated products. Nevertheless, a number of human neural stem cell lines have been developed as in vitro model systems for studying neurogenesis. Hence, we utilized two commercially available neural stem cell lines, ENStem-A cell [13] and ReNcell VM [14], to monitor the expression of ACD protein complexes during differentiation. ENStem-A cell is derived from a National Institutes of Health (NIH)-approved H9 human embryonic stem cell and it has been utilized in cell transplantation experiments on stroke-damaged rats [15]. ReNcell VM is derived from the ventral mesencephalon region of human fetal brain tissue. Different from ENStem-A^{TM} cell, this cell line is immortalized by retroviral transduction with the v-myc oncogene and it can be propagated for 45 passages before losing the ability to differentiate. ReNcell VM has been employed to study the effects of microRNA [16] as well as key signaling pathways [17,18] on neuronal differentiation. By utilizing these cell lines, we revealed an upregulation of components of the spindle orientation complex during neuronal differentiation and demonstrated the specificity of molecular interactions of G protein subunits within the complex.

2. Results

2.1. Expression Profile of ACD-Related Proteins during Differentiation

Prior to examining the expression profile of ACD-related proteins, we first characterized the differentiation capability of the two neural progenitor cell lines. Nestin and Sox-2 were utilized as markers for the pluripotency status while β-III tubulin served as a marker for differentiated neuronal cells. ENStem-A and ReNcell VM cells in early passage (around 6th to 9th passage after thawing) were induced to undergo differentiation for 10 days. Cells were harvested and lysed immediately upon initiation of differentiation (Day 0) or after culturing for 3, 7 or 10 days in the differentiation medium. The expressions of nestin and Sox-2 decreased over the course of differentiation in both cell lines (Figure 1A). The expression of Sox-2 was markedly reduced by Day 7, while the level of nestin became almost undetectable by Day 10. In contrast, the expression of β-III tubulin as a neuronal marker increased noticeably by Day 7 and beyond (Figure 1A). The down-regulation of nestin and Sox-2 with the concomitant appearance of β-III tubulin upon differentiation of the neural progenitor cells were further confirmed by confocal microscopy. As illustrated in Figure 1B, undifferentiated ENStem-A cells typically express Sox-2 but not β-III tubulin. Upon incubation of ENStem-A cells in the differentiation medium for 7 days, Sox-2 immunoreactivity was greatly reduced while those of β-III tubulin became clearly detectable (Figure 1B) , while the presence of glial fibrillary acidic protein was undetectable or negligible. Likewise, the expression of nestin in ReNcell VM became undetectable by Day 7 of differentiation, whereas β-III tubulin immunoreactivity appeared in the differentiated cells (Figure 1C). Under the conditions used, ReNcell VM would generate dopaminergic neurons and we indeed observed the appearance of tyrosine hydroxylase by Day 7 of differentiation (data not shown). These results indicate that a substantial proportion of the cell population underwent differentiation.

Polarity proteins and spindle orientation proteins were then examined by Western blots during the differentiation of both neural progenitor cell lines. The expression of polarity proteins, namely aPKC, Par3, and Par6 in ENStem-A cells remained largely unchanged throughout the 10 days of differentiation (Figure 2A). Although variations in the levels of some target proteins were detected in independent experiments (e.g., elevated aPKC on Day 7 as shown in Figure 2A), such observations were not consistently reproduced. Likewise, no significant alterations in the levels of polarity proteins could be reproducibly detected in ReNcell VM cells over the 10-day differentiation period (Figure 2A). In contrast, several components of the spindle orientation protein complex were upregulated in both ENStem-A and ReNcell VM cells during the course of their differentiation (Figure 2B). NuMA was upregulated by Day 3 and it remained high throughout the differentiation of ENStem-A cells, while its upregulation appeared to be slower in ReNcell VM cells (Figure 2B). Even though it has been suggested that $G\alpha_{i3}$ subunit is responsible for ACD [19], the identity of the $G\alpha_i$ subunit involved in the spindle orientation complex has not been unequivocally established. Thus, we examined the expression of all three isoforms of the $G\alpha_i$ protein by specific antisera. $G\alpha_{i1}$ and $G\alpha_{i2}$ were weakly expressed in ENStem-A cells but they were apparently up-regulated after 7 days of differentiation, whereas $G\alpha_{i3}$ was more abundantly expressed with no change in its level throughout the differentiation (Figure 2B). Similar results were obtained with the ReNcell VM cells (Figure 2B). As the spindle orientation complex can be formed with either AGS3 or LGN, we monitored the expression of both proteins during the differentiation of the neural progenitor cell lines. AGS3 and LGN were both weakly expressed in ENStem-A cells and their levels were slightly elevated upon differentiation for 7 days or more (Figure 2B). Increased expressions of AGS3 and LGN were more discernable in ReNcell VM cells (Figure 2B). Expression of the ankyrin protein mInsc was not altered during the differentiation of ENStem-A or ReNcell VM cells (Figure 2B). Because some of the changes in target protein levels were rather subtle, immunoblots from multiple independent experiments were analyzed by densitometric scanning. As shown in Figure 2C, the levels of $G\alpha_{i2}$, NuMA, AGS3, and LGN were significantly elevated in ENStem-A cells upon differentiation for 7 days or more.
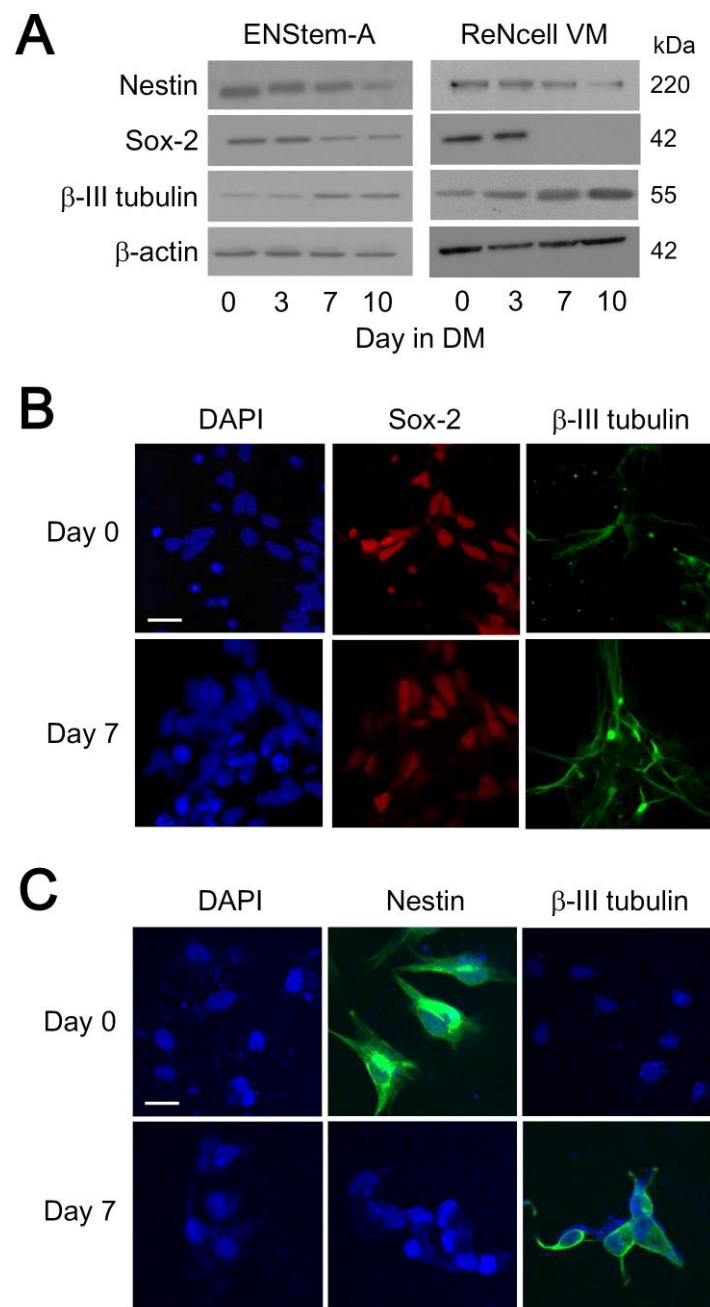
Figure 1. Differentiation of human neural progenitor cells. (**A**) ENStem-A cells were induced to undergo differentiation at passage number 6 while ReNcell VM cells were induced at passage number 9. Cell lysates were collected at Day 0, Day 3, Day 7 and Day 10 of differentiation and subjected to Western blot analysis using anti-Nestin, anti-Sox-2, anti-β-III tubulin and anti-β-actin antisera. Data shown represent one of three or more sets of immunoblots; other sets yielded similar results. (**B**) ENStem-A cells were fixed by 4% paraformaldehyde at Day 0 and Day 7 of differentiation. Cell nuclei were stained with DAPI (4′,6-diamidino-2-phenylindole) while Sox-2 and, β-III tubulin were identified by specific antisera and fluorescent secondary antibodies. Images were obtained with a Zeiss LSM700 confocal microscope. (**C**) ReNcell VM cells were processed as in B except anti-nestin was used instead of anti-Sox-2 for assessing pluripotency. Scale bar indicates 10 μm.
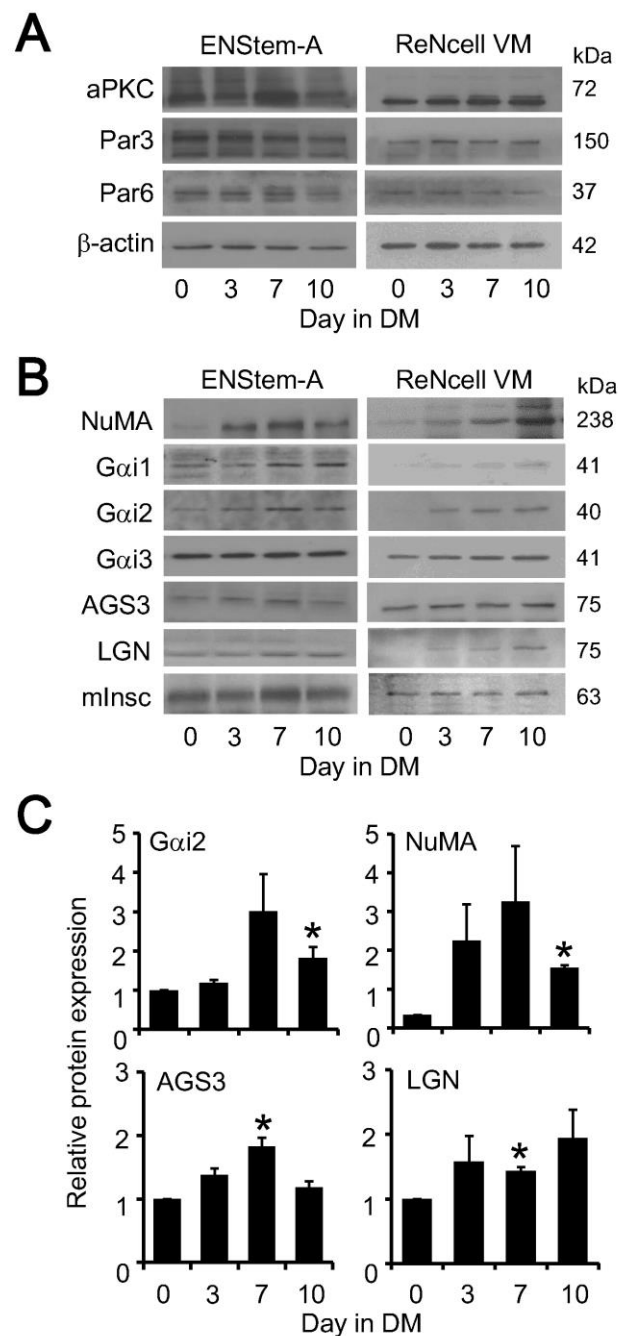
Figure 2. Upregulation of spindle orientation proteins in human neural progenitor cells during differentiation. ENStem-A and ReNcell VM cells were induced to undergo differentiation. Cell lysates were collected at Day 0, Day 3, Day 7 and Day 10 of differentiation. (**A**) Expression of polarity proteins were determined by Western blot analysis using anti-atypical protein kinase C (aPKC), anti-partition defective 3 (Par3), anti-Par6 and anti-β-actin antisera. (**B**) Expression of spindle orientation proteins were assessed by Western blot analysis using anti-nuclear mitotic apparatus (NuMA), anti-Gα_{i1}, anti-Gα_{i2}, anti-Gα_{i3}, anti-AGS3, anti-LGN and anti-inscuteable antisera; please see β-actin immunoreactivity in panel A for reference protein expression. Data shown represent one of three or more sets of immunoblots; other sets yielded similar results. (**C**) Quantitative analysis of the expression of Gα_{i2}, NuMA, AGS3 and LGN using the ImageJ software. Data were expressed as the mean ± S.E. of at least three independent sets of experiments. The probability of an observed difference being a coincidence was evaluated by Dunnett t test. Differences at values of $p < 0.05$ were considered significant (* $p < 0.05$).

We further used confocal imaging to examine how the expression and localization of these spindle orientation protein components changed during differentiation of ENStem-A cells. Indeed, more NuMA, LGN and AGS3 were detected at Day 7 as compared to Day 0 of differentiation, with LGN and AGS3 distributed throughout the cell and NuMA mainly found in the nucleus (Figure 3A). Co-localization of NuMA and LGN in cell nuclei was observed at Day 7 (Figure 3B). To investigate whether the protein expression changes were due to transcriptional or translational regulation, mRNA expression of each of the protein were checked by RT-PCR. The transcripts for all three $G\alpha_i$ subunits and LGN remained essentially unchanged during differentiation, whereas the mRNA of AGS3 was transiently elevated at Day 7 and elevation of NuMA mRNA was detected from Day 3 onwards (Figure 3C). These results imply that the upregulation of spindle orientation proteins may be tightly correlated with the differentiation of neural progenitor cells.

To confirm that the spindle orientation proteins were indeed assembled as a complex during neuronal differentiation, co-immunoprecipitation experiment was performed in ENStem-A cells before and after differentiation for 7 days using AGS3 as the prey; AGS3 is preferred over LGN because it is restrictively expressed in neurons. Cell lysates with equivalent amount of AGS3 were subjected to immunoprecipitation with an anti-AGS3 antiserum and the precipitates probed with antisera against $G\alpha_{i2}$, $G\alpha_{i3}$, or NuMA. Although $G\alpha_{i2}$ was clearly present in the cell lysates of Day 0 and Day 7 samples, it could not be detected in the AGS3 immunoprecipitates (Figure 3D). In contrast, $G\alpha_{i3}$ was co-immunoprecipitated by anti-AGS3 after 7 days of differentiation but not on Day 0 (Figure 3D). Consistent with Figure 2B, NuMA was upregulated upon differentiation of ENStem-A cells and, like $G\alpha_{i3}$, it was co-immunoprecipitated by anti-AGS3 (Figure 3D). These results indicate the formation of the AGS3/$G\alpha_{i3}$/NuMA spindle orientation complex upon differentiation of neural progenitor cells.

2.2. Interaction between $G\alpha_i$ Subunits and AGS3

The preceding experiments revealed the upregulation of spindle orientation proteins during the differentiation of neural progenitor cells. The preferential interaction of AGS3 with $G\alpha_{i3}$ is rather intriguing since $G\alpha_i$ subunits share 85% sequence identity. Hence, we further examined the specificity of interactions among the spindle orientation proteins. To overcome the scarcity and difficulties in handling the neural progenitor cell lines, HEK293 cell was used as a model system to study protein–protein interactions by performing a series of co-immunoprecipitation experiments. HEK293 cells were transiently co-transfected with cDNAs encoding a GST-tagged AGS3 and one of the three $G\alpha_i$ subunits, and the transfectants were subsequently subjected to immunoprecipitation with an anti-GST antibody. Among the three $G\alpha_i$ subunits examined, both $G\alpha_{i2}$ and $G\alpha_{i3}$ were detected in the anti-GST immunoprecipitates with the latter exhibiting the strongest interaction with AGS3 (Figure 4A); $G\alpha_{i1}$ failed to associate with AGS3 despite obvious overexpression of $G\alpha_{i1}$ in the cell lysates of the transfectants (Figure 4A). These results suggest that AGS3 can distinguish between the different $G\alpha_i$ subunits. Since AGS3/LGN are known to preferably bind to GDP-bound $G\alpha_i$ subunits [8], the interaction between $G\alpha_{i3}$ and AGS3 might be stabilized in the presence of the non-hydrolyzable GDPβS but weakened by GTPγS. In transfectants transiently co-expressing GST-AGS3 and $G\alpha_{i3}$, treatment of the cell lysates with GTPγS (100 μM for 6 h at 4 °C) greatly reduced the amount of $G\alpha_{i3}$ that was co-immunoprecipitated by the anti-GST antibody, whereas GDPβS treatment appeared to stabilize the formation of AGS3/$G\alpha_{i3}$ as the level of $G\alpha_{i3}$ found in the precipitates was identical to that of the control sample (Figure 4B, middle panels). Similar results were obtained with HEK293 cells co-expressing GFP-tagged LGN and $G\alpha_{i3}$ (Figure 4B, right hand panels). In contrast, AGS3 failed to pull down $G\alpha_{i2}$ from the cell lysates of transfectants co-expressing GST-AGS3 and $G\alpha_{i2}$ (Figure 4B, left hand panels).
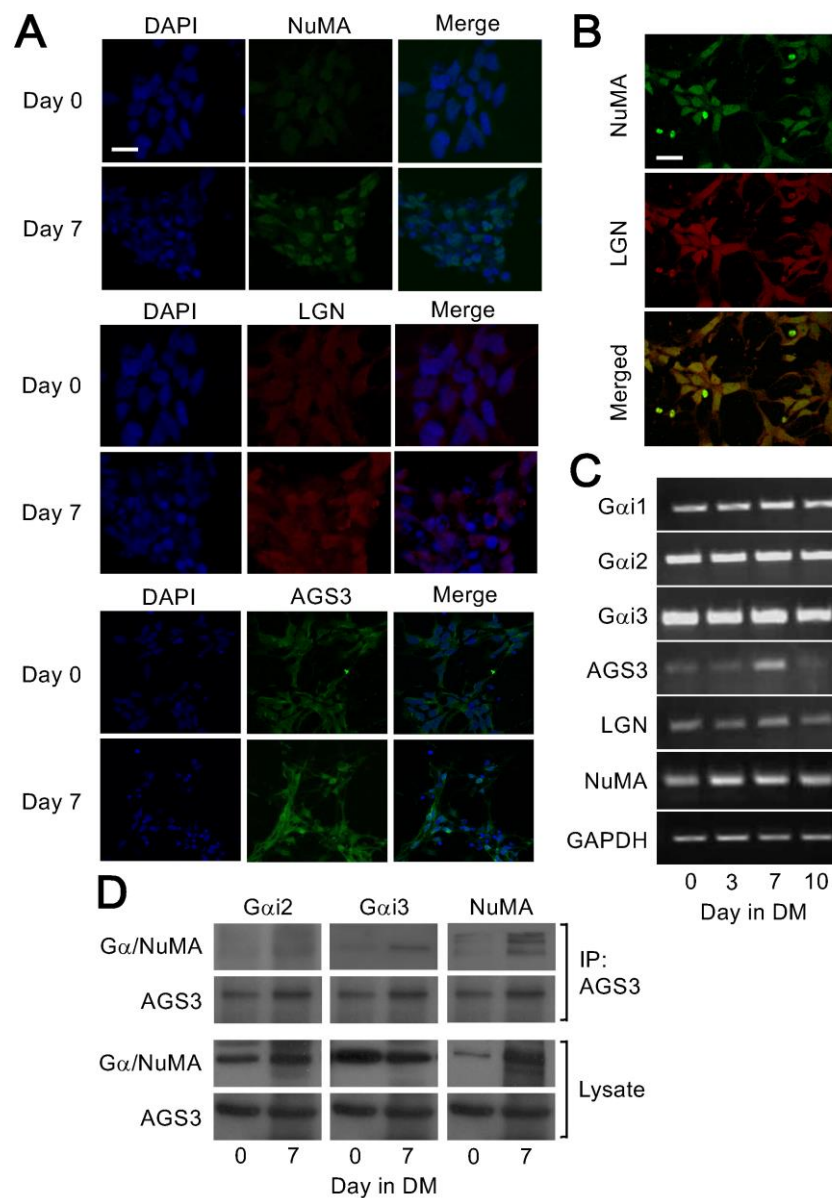
Figure 3. Co-localization and complex formation by upregulated spindle orientation proteins during differentiation of ENStem-A cells. (**A**) ENStem-A cells were fixed by 4% paraformaldehyde at Day 0 and Day 7 of differentiation. Cell nuclei were stained with DAPI and the presence of NuMA, LGN, and AGS3 detected by fluorescence staining using specific antisera. Images were obtained with a Zeiss LSM700 confocal microscope. Scale bar indicates 10 μm. (**B**) Images of LGN and NuMA at Day 7 were merged (bottom panel) to illustrate their co-localization. Scale bar indicates 10 μm. (**C**) ENStem-A cells were induced to undergo differentiation and total RNA was extracted using RNeasy Mini kit (Qiagen) at Day 0, Day 3, Day 7 and Day 10. Each RNA sample was then subjected to reverse transcription to generate cDNA followed by PCR amplification with primers corresponding to $G\alpha_{i1}$, $G\alpha_{i2}$, $G\alpha_{i3}$, AGS3, LGN, NuMA and GAPDH. (**D**) ENStem-A cells were induced to undergo differentiation and cell lysates were collected at Day 0 and Day 7 of differentiation. Samples were incubated with anti-AGS3 antisera and then immunoprecipitated using protein G agarose. Presence of $G\alpha_{i2}$, $G\alpha_{i3}$ and NuMA in the immunoprecipitates (IP) and cell lysates were detected by Western blotting with specific antisera.
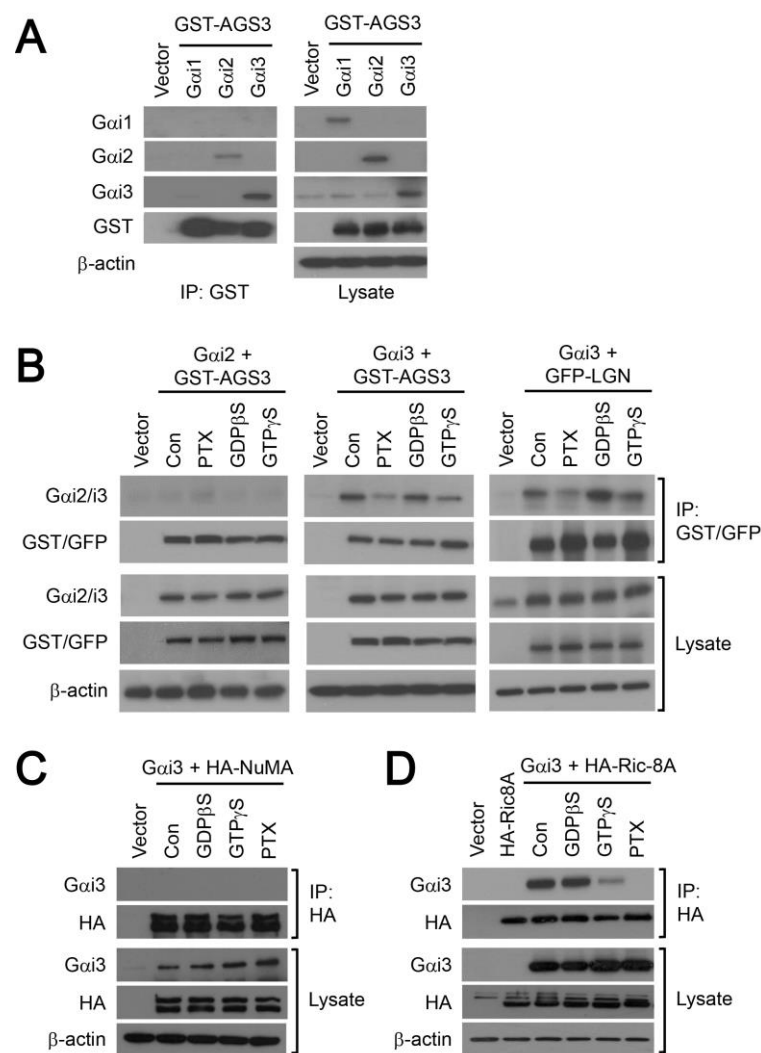
Figure 4. Interaction of Gα$_i$ with components of the spindle orientation complex in HEK293 cells. (**A**) HEK293 cells were transiently transfected with vector (pcDNA3.1), or co-transfected with GST-tagged AGS3 and Gα$_{i1}$, Gα$_{i2}$ or Gα$_{i3}$. Samples were incubated with anti-GST and then immunoprecipitated using protein G agarose. Presence of Gα$_{i1}$, Gα$_{i2}$, Gα$_{i3}$ and GST-tagged AGS3 were analyzed by Western blotting with specific antisera. (**B**) HEK293 cells were transiently transfected with vector (pcDNA3.1), or co-transfected with GST-tagged AGS3 or GFP tagged LGN and Gα$_{i2}$ or Gα$_{i3}$. One day after transfection, cells was treated with or without pertussis toxin (PTX) for 16 h. Cell lysates were subjected to treatment with GDPβS and GTPγS (100 μM; 6 h at 4 °C). Samples were subjected to immunoprecipitation with either anti-GST or anti-GFP antisera and protein G agarose. Gα$_i$ subunits in the immunoprecipitates were detected by Western blot analysis. (**C**) HEK293 cells transiently co-expressing HA-tagged NuMA and Gα$_{i3}$ were subjected to co-immunoprecipitation with anti-HA agarose and Western blotting as in **B**. (**D**) HEK293 cells were treated as in *C* except that HA-tagged Ric-8A was transfected and probed instead of HA-tagged NuMA.

Recent structural studies have revealed that the Gα$_i$ subunits bind to the four GoLoco motifs on AGS3/LGN through their switch I-III regions [20,21]. Since these regions are essential for the Gα$_i$ to interact productively with GPCRs, Gβγ dimer, and effectors [22], their occupation by AGS3 is likely to displace other binding partners of Gα$_i$. Conversely, the formation of AGS3/Gα$_i$ complexes might be enhanced by limiting the ability of Gα$_i$ to recognize its binding partners. GPCRs are the canonical and predominant partners of G$_i$ proteins and their functional association can be abolished upon pertussis toxin (PTX)-catalyzed ADP-ribosylation of the Gα$_i$ subunit. Hence, we examined

the effect of PTX treatment (100 ng/mL, 16 h) on the ability of GST-AGS3 or GFP-LGN to pull down $G\alpha_{i3}$ in HEK293 transfectants. Interactions between $G\alpha_{i3}$ and both AGS3 and LGN were diminished following PTX treatment (Figure 4B, middle and right hand panels), indicating that the attachment of an ADP-ribose group on the C-terminus of $G\alpha_{i3}$ disrupted the binding to AGS3/LGN. To further demonstrate the specificity of AGS3/$G\alpha_{i3}$ interaction in an overexpression system, we asked if $G\alpha_{i3}$ could be co-immunoprecipitated by NuMA and Ric-8A (a guanine nucleotide exchange factor or GEF of $G\alpha_i$). In the spindle orientation complex, NuMA is bound to AGS3 but not $G\alpha_i$ [5] and thus it is not expected to form a complex with $G\alpha_{i3}$ in the absence of AGS3. Co-expression of HA-tagged NuMA with $G\alpha_{i3}$ and subsequent immunoprecipitation with an anti-HA antibody failed to detect $G\alpha_{i3}$ in the precipitates irrespective of pretreatments with guanine nucleotides of PTX (Figure 4C). Replacement of HA-NuMA by HA-Ric-8A in similar experiments resulted in the co-immunoprecipitation of $G\alpha_{i3}$ with Ric-8A (Figure 4D). This is in line with a previous study which suggests that Ric-8A together with $G\alpha_i$ are crucial in recruiting other components in the spindle orientation complex to the cell cortex for proper mitotic spindle orientation [10]. Like AGS3, the association of Ric-8A with $G\alpha_{i3}$ was sensitive to GTPγS and PTX treatments (Figure 4D); failure of Ric-8A to form a complex with ADP-ribosylated $G\alpha_i$ has been previously demonstrated [10]. These studies suggest that heterologous expression of $G\alpha_{i3}$ with its binding partners such as AGS3 and Ric-8A can generate detectable complexes in HEK293 cells.

3. Discussion

Most of the mechanistic insights on ACD are derived from studies on invertebrate systems that allow in vivo monitoring of neurogenesis. Although imaging technology has advanced to a stage where it is now possible to broadly examine adult hippocampal neurogenesis in mice, it remains extremely challenging to follow the fate of specific cell lineages, let alone to determine the dynamic changes associated with the assembly and function of protein complexes. Our current understanding on ACD is largely based on studies in invertebrates such as *Drosophila* and *C.elegans* [6]. The existence of mammalian cell polarity and spindle orientation complexes have been extensively documented in studies utilizing recombinant proteins, and their putative functions demonstrated in several experimental systems such as epithelial cells that exhibit cell polarity [23–25]. Yet, the precise functions of these protein complexes in regulating ACD of neural progenitor cells are not fully understood. The use of two human neural progenitor cell lines in the present study enabled us to monitor the abundance of individual components that constitute the cell polarity and spindle orientation complexes. As the levels of Par3, Par6 and aPKC did not alter substantially during the 10-day differentiation period of both ReNcell VM and ENStem-A cells (Figure 2A), formation of the polarity complex with pre-existing components is apparently sufficient to support neurogenesis. In contrast, elevated expressions of all three components of the spindle orientation complex were detected towards the latter half of differentiation (Day 7 and Day 10) of the neural progenitor cells (Figure 2B), which coincided with the appearance of the neuronal marker β-III tubulin (Figure 1). Moreover, increased transcript levels of these components were observed in ENStem-A cells and the upregulated proteins were co-localized and capable of forming more complexes during differentiation (Figure 3). These results suggest that, unlike the polarity complex, pre-existing components may not be sufficient to ensure proper assembly of the spindle orientation complex during neurogenesis.

Neuronal differentiation and neurogenesis are intricately associated in order to generate new mature neurons. Instead of examining the effects of spindle orientation proteins on the process of ACD, our focus is placed on the assembly of the spindle orientation complex. Our data suggest that the formation of spindle orientation complex may be dynamically controlled during the differentiation of neural progenitor cells. Although all three components of the spindle orientation complex were upregulated upon differentiation of ReNcell VM and ENStem-A cells, elevation of NuMA was most easily detectable (Figure 2B). Co-immunoprecipitation data demonstrate that increased expression of NuMA during differentiation of ENStem-A cells can lead to the formation of additional complexes with AGS3 and $G\alpha_{i3}$ (Figure 3D). The precise composition of the spindle orientation complex, however,

remains equivocal as both AGS3 and LGN are capable of interacting with NuMA and various $G\alpha_i$ subunits [25–27]. We used AGS3 primarily in the present study because its expression is restricted to neurons, whereas LGN is expressed in neuronal, astroglial, and microglial cultures [28]. It should be noted that an upregulation of AGS3 has been reported in differentiating human neural progenitor cells [29]. Although LGN appears to be involved in regulating spindle orientation during ACD [29], an alternative mechanism involving AGS3 regulating spindle positioning has also been proposed [26]. The mechanisms by which the components of the spindle orientation complex are upregulated have yet to be explored as both transcriptional and post-transcriptional processes may be involved. However, it should also be noted that increased expression of NuMA and AGS3 may not be exclusively associated with the establishment of spindle pole orientation because they possess additional functions; NuMA is apparently required for the selective induction of p53 genes [30] while the GoLoco (or G protein regulatory) motifs of AGS3 is critical for regulating cytokine production [31].

One of the unresolved issues regarding the spindle orientation complex in human neural progenitor cells pertains to the identity of the $G\alpha_i$ subunit. Unlike *Drosophila* and *C. elegans* that only express one isoform of $G\alpha_i$, mammalian genomes encode three different $G\alpha_i$ subunits with 85–95% amino acid sequence identity. The $G\alpha_{i1\text{-}3}$ share the same ability to inhibit adenylyl cyclase [32] and have partially overlapping expression patterns [33]. $G\alpha_{i2}$ is expressed ubiquitously and represents the quantitatively predominant $G\alpha_i$ isoform, but its expression is often accompanied by $G\alpha_{i1}$ and/or $G\alpha_{i3}$. All three subtypes of $G\alpha_i$ were detected in both ReNcell VM and ENStem-A cells, albeit $G\alpha_{i3}$ was more abundantly expressed. Although the levels of both $G\alpha_{i1}$ and $G\alpha_{i2}$ increased upon differentiation of the neural progenitor cells (Figure 2B), AGS3 appeared to preferentially bind $G\alpha_{i3}$ in ENStem A cells (Figure 3D). The high abundance of $G\alpha_{i3}$ might account for the lack of a detectable AGS3/$G\alpha_{i2}$ complex in ENStem-A cells, because weak association of $G\alpha_{i2}$ with AGS3 could be detected in transfected HEK293 cells (Figure 4A); the weaker interaction between AGS3 and $G\alpha_{i2}$ further suggests a preference of $G\alpha_{i3}$ by AGS3. A similar observation has also been reported in a study using mouse cerebral cortical progenitors, where AGS3 preferentially binds to $G\alpha_{i3}$ instead of $G\alpha_{i1}$ and $G\alpha_{i2}$ [26]. Given the high sequence similarity and functional resemblance of the $G\alpha_i$ subunits, it is difficult to comprehend why AGS3 prefers $G\alpha_{i3}$. The inability of $G\alpha_{i1}$ to interact with AGS3 in both ENStem-A (Figure 3D) and transfected HEK293 (Figure 4A) cells is especially intriguing, because it shares 95% amino acid sequence identity with $G\alpha_{i3}$ [34]. Perhaps the answer lies in their differential availability within the intracellular compartments. It is noteworthy that, amongst the different $G\alpha$ subunits, $G\alpha_{i3}$ is the one most often detected in subcellular compartments in addition to its typical localization at the plasma membrane. $G\alpha_{i3}$ is present on the cytoplasmic face of the Golgi cisternae [35], autophagosomes [36], and endocytic compartments [37], which may be associated to its non-canonical signaling functions in the control of cell differentiation [38,39] and autophagy [40]. Alternatively, the preference of AGS3 for $G\alpha_{i3}$ may be dictated by other proteins that show selectivity for either or both protein partners. Unequivocal demonstration of the specificity of $G\alpha_{i3}$ for AGS3 may require knockdown of the different $G\alpha_i$ subunits. However, attempts to knockdown $G\alpha_i$ subunits in neural progenitor cells resulted in non-viable cells (unpublished observations), while similar manipulations in HEK293 cells led to compensatory changes in the expression of G protein subunits [41].

Another interesting observation which deserves further discussion is the inability of ADP-ribosylated $G\alpha_i$ to form complexes with AGS3, since PTX treatment is generally believed to have no effect on the function of AGS3 [42,43]. PTX targets the cysteine residue four amino acids from the C-terminus of $G\alpha_i$ for ADP-ribosylation. The attachment of a bulky ADP-ribose group to the carboxyl α5 helix is known to prevent receptor recognition by the modified $G\alpha_i$ subunit. Yet, as revealed by molecular modeling, the GoLoco motifs of AGS proteins bind to the switch II region of the $G\alpha_i$ subunit [20,21] which is located on a plane different from the cysteine targeted by PTX (Figure 5A). The binding of the GoLoco motif on the $G\alpha_i$ effectively prevents the latter from associating with Gβγ (Figure 5B) and thus provides a structural basis for the AGS proteins to primarily bind to Gβγ-dissociated $G\alpha_i$ subunits [44]. The free $G\alpha_i$ resulted from formation of the AGS3/$G\alpha_i$ complex has

been proven to be crucial in regulating spindle orientation as impairing Gβγ signaling and silencing AGS3 both disrupt the spindle orientation during ACD [26]. Yet, it is difficult to comprehend how ADP-ribosylation can impair the association of AGS3 to the Gα$_i$ subunit. A plausible explanation may be related to the mechanism of ADP-ribosylation by PTX. Early studies have shown that PTX recognizes the heterotrimeric G$_i$ proteins rather than the dissociated Gα$_i$ subunit [45]. Since ADP-ribosylated G$_i$ proteins cannot be stimulated by GPCRs, the generation of Gβγ-dissociated Gα$_i$ subunits will diminish as the ADP-ribosylation reaction proceeds with time. With limited availability of free Gα$_i$ subunits, formation of the AGS3/Gα$_i$ complex will be impeded (Figure 4B). Inhibition of the binding of AGS3 to Gα$_i$ by PTX was typically more extensive than that observed with GTPγS (Figure 4B). This may be attributed to mechanistic differences and distinct experimental conditions wherein the incubation time for GTPγS was substantially shorter (6 h versus 16 h). Alternatively, the C-terminal tail of Gα$_i$ may represent another contact site for AGS3 because the current structural model of the AGS3/Gα$_i$ complex is based on the GoLoco motif rather than the entire AGS3/LGN molecule [20,21]. This possibility cannot be discarded without resolving the complete structure of the AGS3/Gα$_i$ complex. Since the PTX site on Gα$_i$ is critical for receptor recognition, AGS3 binding to this site may result in competition with receptors for Gα$_i$ subunits to modulate receptor signaling function. Such a scenario is highly likely in view of the recent demonstration of AGS3 forming a chemokine regulated, Gα$_i$-dependent complex with CXCR4 and CCR7 receptors [46]. Indeed, there is substantial evidence in support of the notion that the Gα$_i$-AGS3 complex is in close proximity to GPCRs and can regulate receptor signaling [47,48]. Possible involvement of GPCRs in regulating neurogenesis is further highlighted by the identification of numerous orphan GPCRs in neural stem cells including the ReNcell VM and ENStem-A cells [49].
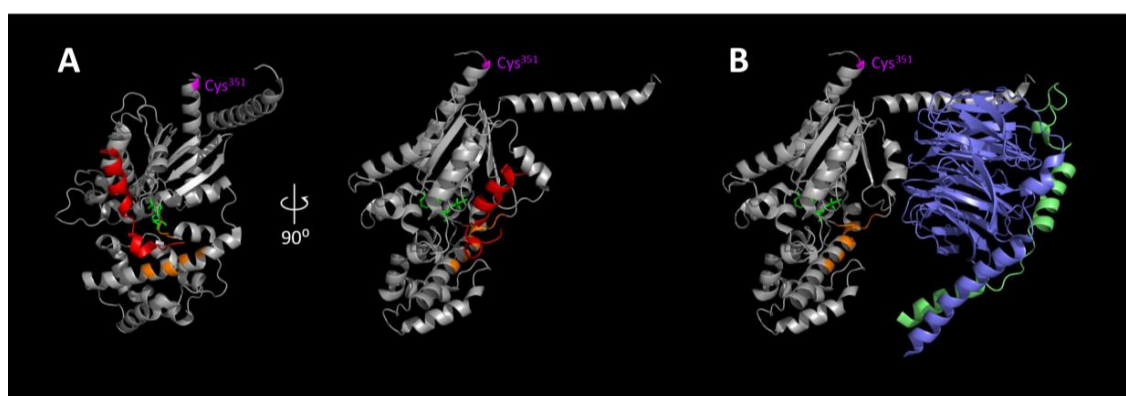

Figure 5. Crystal structures of Gα$_i$-GDP in complex with GoLoco motif or Gβγ subunits. (**A**) Ribbon diagram of the Gα$_i$-GDP in complex with GoLoco motif crystal structure in two views related by a 90° rotation about the vertical axis. The model of a full length Gα structure (residues 5-354) was constructed by combining published crystal structures of Gα$_i$ subunits (PDB entries 4G5R and 1GP2). Selected amino acids suggested to participate in GoLoco motif interaction (Tyr[69], Val[72], Ser[75], Gln[79], Val[179] and Thr[181]; Jia et al., 2012) are highlighted in *orange*. Gα$_i$ and GoLoco peptide are shown in *light gray* and *red*, respectively. The PTX ADP-ribosylation site (Cys[351]) is highlighted in *magenta*. GDP is shown in the ball-and-stick model (*green*). (**B**) Ribbon diagram of the Gα$_i$-GDP in complex with Gβγ subunits crystal structure. Gβ and Gγ subunits are shown in *blue* and *lime*. The color scheme of Gα$_i$ is the same as in **A**.

Despite the general consensus that AGS3 selectively interacts with GDP-bound Gα$_i$ subunits in the absence of the Gβγ dimers, the question of how GDP•Gα$_i$ subunits are generated has not been unequivocally resolved. Activation of G$_i$ proteins by a GEF will lead to the binding of GTP by Gα$_i$ subunits and the concomitant release of Gβγ dimers. Intrinsic GTPase activity of the Gα$_i$ subunit ensures the eventual hydrolysis of GTP to GDP and the resulting GDP•Gα$_i$ subunits will then be available for binding by AGS3, provided that the latter can successfully compete against the Gβγ dimers. Such a mechanism is postulated to facilitate the formation of the spindle orientation complex, and the

GEF is presumed to be Ric-8A because of its ability to associate with the spindle orientation complex [50]. However, the demonstration of Ric-8A acting as a GEF for G_i proteins was performed with recombinant proteins [50,51] and no such activity could be observed under in cellulo conditions [52]. It would seem that Ric-8A may not be the actual GEF that generates GDP•$G\alpha_i$ subunits endogenously for the formation of the spindle orientation complex. Given that GPCRs can directly associate with AGS3 [47], they are well positioned to supply GDP•$G\alpha_i$ subunits for AGS3. In this regard, it is noteworthy that several orphan GPCRs have significant effects on neurogenesis. GPR85, also known as the super conserved receptor expressed in brain 2 (SREB2), negatively regulates neurogenesis in the mouse hippocampus [53], whereas GPRC5B (G protein-coupled receptor class C 5B) appears to contribute to neurogenesis in the developing mouse neocortex [54], and Tre1 (Trapped in endoderm 1) orientates stem cell divisions through the spindle orientation and polarity complexes in the *Drosophila* [55]. In line with these recent studies supporting the possible involvement of GPCRs in neurogenesis, expression of GPR85 in ENStem-A cells is downregulated upon differentiation for 10 days (unpublished data). If orphan GPCRs are indeed involved in regulating the formation of spindle orientation complexes, their successful deorphanization may offer new avenues to manipulate neurogenesis.

While overexpressing different proteins involved in spindle orientation in HEK293 cell enables us to decipher the specific molecular organization of the protein complex, it is interesting to investigate the effect of disrupting interactions between heterotrimeric G protein and GPCRs/AGS3 on neurogenesis of human neural progenitors. One of potential future direction is to look at the spindle positioning when the human progenitor cell undergoes ACD. However, it is important to note that the use of PTX on neural progenitor cells may mask the investigation on structural interaction as it inhibits other GPCR-mediated pathways such as the phosphorylation of extracellular-signal regulated kinase that promotes cell proliferation and mitogen-activated protein kinase that leads to cell migration in human neural progenitor cells [56,57].

In summary, the present study revealed that the components of the spindle orientation complex are upregulated upon differentiation of human neural progenitor cells. Although several types of $G\alpha_i$ subunits are endogenously expressed in human neural progenitor cells, $G\alpha_{i3}$ appeared to be the preferred partner of AGS3 in the complex. Disruption of the AGS3/$G\alpha_{i3}$ interaction by PTX further raised mechanistic implications in the formation of the spindle orientation complex. It is important to delineate the signals or conditions that direct GDP•$G\alpha_i$ subunits to associate with AGS3 rather than GEFs that are abundantly expressed, and human neural progenitor cell lines may represent useful models for such endeavors.

4. Materials and Methods

4.1. Materials

The cDNAs of various human $G\alpha$ subunits and AGS3 were purchased from the Missouri S&T cDNA Resource Center. HA-tagged mouse Ric-8A was kindly provided by Dr. Yijuang Chern (National Yang-Ming University). Cell culture reagents, including LipofectAMINE PLUS reagents were purchased from Invitrogen (Carlsbad, CA, USA). Anti-Sox-2 (AB5603), anti-β-III tubulin (MAB1637), anti-Par3 (07-330), anti-inscuteable (ABT64) and anti-nestin (MAB5326) antibodies were from Millipore (Darmstadt, Germany). Anti-β-actin (sab5500001) and anti-HA agarose (A2095) were obtained from Sigma-Aldrich (St. Louis, MO, USA). Antisera against $G\alpha_{i1}$ (sc-13533), $G\alpha_{i2}$ (sc-7276), $G\alpha_{i3}$ (sc-262), aPKC (sc-216), AGS3 (sc-33222), Par6 (sc-25525) and GFP (sc-8334) were purchased from Santa Cruz Biotechnology (Santa Cruz, CA, USA). Anti-NuMA antibody (ab97585) was from Abcam (Cambridge, UK). Anti-GPSM2/LGN (PAB7195) was from Abnova (Taipei City, Taiwan). Anti-GST (#2625) antibody was purchased from Cell Signaling Technology (Danvers, MA, USA). GDPβS and GTPγS were from Calbiochem (San Diego, CA, USA). Protein G agarose was purchased from Roche Diagnostics (Indianapolis, IN, USA).

4.2. Cell Culture

ENStem-A and ReNcell VM were purchased from Millipore (Darmstadt, Germany). For culturing ENStem-A cell, plates were coated with 20 μg/mL poly-ʟ-ornithine in sterilized water for 1 h and then coated with 5 μg/mL laminin in phosphate buffer solution (PBS) for another hour. Cells were maintained with ENStem-A expansion medium supplemented with 20 ng/mL fibroblast growth factor 2 (FGF-2) and 2 mM ʟ-glutamate. For culturing ReNcell VM, plates were coated with 20 μg/mL laminin in Dulbecco's Modified Eagle's Medium with F12 for at least 4 h. They were maintained with ReNcell maintenance medium supplemented with 20 ng/mL of FGF-2 and epithelial growth factor 2 (EGF-2). HEK293 cells were obtained from the American Type Culture Collection (CRL-1573; Rockville, MD, USA) and maintained in Eagle's minimum essential medium (HEK293) at 5% CO_2, 37 °C with 10% fetal bovine serum, 50 units/mL penicillin and 50 μg/mL streptomycin.

4.3. Transfection of HEK293 Cell

HEK293 cells were seeded into 6-well plates at 5×10^5 cells/well in culture medium the day before transfection. Various cDNAs at a concentration of 0.5 μg/well were transiently transfected into the cells using LipofectAMINE PLUS reagents following the supplier's protocol. For co-immunoprecipitation assay, HEK293 cells were seeded into 100 mm culture plates and cultured to 60–80% confluence. Various cDNAs at a total concentration of 8 μg/plate were transiently transfected into the cells using LipofectAMINE PLUS reagents [58].

4.4. Differentiation of ENStem-A Cell and ReNcell VM

One day before the start of differentiation, cells were seeded at a density of 5×10^5/mL in 60 mm plates. Day 0 represents the day when the ENStem-A expansion medium was replaced with ENStem-A differentiation medium without FGF-2 supplement, or when ReNcell VM maintenance medium was washed away with PBS and replaced with the maintenance medium without the addition of EGF-2 and FGF-2. On each time point where cell lysates were collected (i.e., Day 0, Day 3, Day 7 and Day 10), cells were lysed in lysis buffer (25 mM Hepes, 0.1% Nonidet *p*-40, 0.5% sodium deoxycholate, 1 mM dithiothreitol, 200 μM Na_3VO_4, 100 μM phenylmethylsufonyl fluoride, 2 μg/mL leupeptin, 4 μg/mL aprotinin, and 0.7 μg/mL pepstatin). Cell lysates were subjected to protein assay by Bio-Rad DC^{TM} protein assay kit in order to obtain samples with a similar protein amount for expression comparison.

4.5. Immunohistochemistry

Briefly, cells were first fixed with 4% paraformaldehyde, then permeabilized in 0.1–1% Triton X-100 in PBS (PBS-T), incubated in blocking buffer (5% bovine serum albumin), and incubated overnight at 4 °C with the following primary antibodies: mouse anti-β-III tubulin, mouse anti-Nestin, rabbit anti-AGS3, rabbit anti-NuMA, rabbit anti-Sox-2, or goat anti-LGN (1:1000). Species-specific Alexa Fluor secondary antibodies (1:1000; Invitrogen, Carlsbad, CA, USA) were used against the corresponding origin of primary antibodies. Cell culture coverslips were mounted on glass slides and stained with DAPI by ProLong Gold Antifade Mountant with DAPI (Invitrogen, Carlsbad, CA, USA). Images were captured by using confocal laser scanning microscope LSM700 (Zeiss, Oberkochen, Germany) as described previously [59].

4.6. Co-Immunoprecipitation Assays

Transfected HEK293 cells were washed with PBS twice. Cells were subsequently lysed in magnesium containing lysis buffer (25 mM HEPES, 50 mM $MgCl_2$, 0.1% Nonidet *p*-40, 0.5% sodium deoxycholate, 1 mM dithiothreitol, 200 μM Na_3VO_4, 100 μM phenylmethylsufonyl fluoride, 2 μg/mL leupeptin, 4 μg/mL aprotinin, and 0.7 μg/mL pepstatin). Cell lysates were incubated with anti-HA affinity agarose gel or specific antisera followed by protein G agarose at 4 °C for 4 h. Immunoprecipitates

were washed with 400 μL RIPA buffer 4 times and resuspended in 1× sample buffer. After boiling for 5 min, samples were subjected to the Western blot analysis.

4.7. Western Blot Analysis

Protein samples were resolved on 12% SDS-polyacrylamide gels and transferred to Osmonics nitrocellulose membrane. Resolved proteins were detected by their specific primary antibodies and horseradish peroxidase-conjugated secondary antisera. The immunoblots were visualized by chemiluminescence with the ECL kit from Amersham (Amersham, UK), and the images detected in X-ray films were quantified by densitometric scanning using the Eagle Eye II still video system (Stratagene, La Jolla, CA, USA). Western blots were quantified using ImageJ software (version 1.80).

4.8. RT-PCR

ENStem-A cells were washed twice with PBS followed by the addition of 500 μL TRIZOL reagent. Total RNA was extracted using the protocol supplied by the RNeasy Mini kit (Qiagen, Hilden, Germany). RNA (1 μg) of each sample was used for cDNA synthesis with random hexamer as primer by the SuperScriptTM III First-Strand Synthesis System (Invitrogen, Carlsbad, CA, USA). The cDNA product (1 μL) was then used in conjunction with 10 pmol of forward and reverse primers for PCR to determine the levels of target transcripts and GAPDH. The primer sequences targeting $G\alpha_{i1}$, $G\alpha_{i2}$, $G\alpha_{i3}$, LGN, AGS3, NuMA and GAPDH are listed in Table 1. PCR (25 cycles each with 95 °C for 30 s, 55 °C for 60 s and 68 °C for 60 s) was carried out using KAPA 2G Fast HS Readymix PCR Kit (KAPA Biosystems, Wilmington, MA, USA). PCR products were then resolved using 1.2% agarose gel and the fragment sizes corresponding to $G\alpha_{i1}$, $G\alpha_{i2}$, $G\alpha_{i3}$, LGN, AGS3, NuMA and GAPDH were 401 bp, 395bp, 355 bp, 498 bp, 308 bp, 581 bp and 206 bp, respectively.

Table 1. Primer sequences used in detecting mRNA expression of corresponding genes by RT-PCR.

Gene	Sequence
$G\alpha_{i1}$	Sense: 5′-GGA GTA AGA TGA TCG ACC GCA-3′ Antisence: 5′-AAG CTG GTA CTC TCG GGA TCT-3′
$G\alpha_{i2}$	Sense: 5′-GAA GTT GCT GCT GTT GGG TG-3′ Antisnese: 5′-GAA GTT GCT GCT GTT GGG TG-3′
$G\alpha_{i3}$	Sense: 5′-GAG CCA TGG GAC GGC TAA AG-3′ Antisnese: 5′-TGG CCA CCT ACA TCA AAC ATC T-3′
LGN	Sense: 5′-GCT GTC TGA CAT TGA CCT CCT-3′ Antisnese: 5′-ACC ACT AGC TTT CGC TTC CC-3′
AGS3	Sense: 5′-ATC TGA GCA TCG CCC AAG AG-3′ Antisnese: 5′-CTC CTT GTG GAA GGT CGT GG-3′
NuMA	Sense: 5′-GGA ACT GGC GAA GAT GAC CA-3′ Antisnese: 5′-AGA TGA CTG GCA AAC TCC CG-3′
GAPDH	Sense: 5′-GGC GTC TTC ACC ACC ATG GAG-3′ Antisnese: 5′-AAG TTG TCA TGG ATG ACC TTG GC-3′

4.9. Statistical Analysis

Data were expressed as the mean ± S.E. of at least three independent sets of experiments. The probability of an observed difference being a coincidence was evaluated by the Dunnett t test. Differences at values of $p < 0.05$ were considered significant.

References

1. Taverna, E.; Gotz, M.; Huttner, W.B. The cell biology of neurogenesis: Toward an understanding of the development and evolution of the neocortex. *Annu. Rev. Cell Dev. Biol.* **2014**, *30*, 465–502. [CrossRef] [PubMed]

2. Shen, Q.; Zhong, W.; Jan, Y.N.; Temple, S. Asymmetric Numb distribution is critical for asymmetric cell division of mouse cerebral cortical stem cells and neuroblasts. *Development* **2002**, *129*, 4843–4853. [PubMed]

3. Shitamukai, A.; Matsuzaki, F. Control of asymmetric cell division of mammalian neural progenitors. *Dev. Growth Differ.* **2012**, *54*, 277–286. [CrossRef] [PubMed]

4. Suzuki, A.; Ohno, S. The PAR-aPKC system: Lessons in polarity. *J. Cell Sci.* **2006**, *119*, 979–987. [CrossRef]

5. Bowman, S.K.; Neumuller, R.A.; Novatchkova, M.; Du, Q.; Knoblich, J.A. The *Drosophila* NuMA homolog Mud regulates spindle orientation in asymmetric cell division. *Dev. Cell* **2006**, *10*, 731–742. [CrossRef] [PubMed]

6. Siller, K.H.; Doe, C.Q. Spindle orientation during asymmetric cell division. *Nat. Cell Biol.* **2009**, *11*, 365–374. [CrossRef]

7. Roubinet, C.; Cabernard, C. Control of asymmetric cell division. *Curr. Opin. Cell Biol.* **2014**, *31*, 84–91. [CrossRef] [PubMed]

8. Du, Q.; Macara, I.G. Mammalian Pins is a conformational switch that links NuMA to heterotrimeric G proteins. *Cell* **2004**, *119*, 503–516. [CrossRef] [PubMed]

9. Konno, D.; Shioi, G.; Shitamukai, A.; Mori, A.; Kiyonari, H.; Miyata, T.; Matsuzaki, F. Neuroepithelial progenitors undergo LGN-dependent planar divisions to maintain self-renewability during mammalian neurogenesis. *Nat. Cell Biol.* **2008**, *10*, 93–101. [CrossRef] [PubMed]

10. Woodard, G.E.; Huang, N.N.; Cho, H.; Miki, T.; Tall, G.G.; Kehrl, J.H. Ric-8A and $G_i\alpha$ recruit LGN, NuMA, and dynein to the cell cortex to help orient the mitotic spindle. *Mol. Cell. Biol.* **2010**, *30*, 3519–3530. [CrossRef]

11. Doze, V.A.; Perez, D.M. G-protein-coupled receptors in adult neurogenesis. *Pharmacol. Rev.* **2012**, *64*, 645–675. [CrossRef] [PubMed]

12. Tse, M.K.; Wong, Y.H. Neuronal functions of activators of G protein signaling. *Neurosignals* **2013**, *21*, 259–271. [CrossRef]

13. Shin, S.; Mitalipova, M.; Noggle, S.; Tibbitts, D.; Venable, A.; Rao, R.; Stice, S.L. Long-term proliferation of human embryonic stem cell derived neuroepithelial cellsing defined adherent culture conditions. *Stem Cells* **2006**, *24*, 125–138. [CrossRef]

14. Hoffrogge, R.; Mikkat, S.; Scharf, C.; Beyer, S.; Christoph, H.; Pahnke, J.; Mix, E.; Berth, M.; Uhrmacher, A.; Zubrzycki, I.Z.; et al. 2-DE proteome analysis of a proliferating and differentiating human neuronal stem cell line (ReNcell VM). *Proteomics* **2006**, *6*, 1833–1847. [CrossRef] [PubMed]

15. Chang, D.J.; Oh, S.H.; Lee, N.; Choi, C.; Jeon, I.; Kim, H.S.; Shin, D.A.; Lee, S.E.; Kim, D.; Song, J. Contralaterally transplanted human embryonic stem cell-derived neural precursor cells (ENStem-A) migrate and improve brain functions in stroke-damaged rats. *Exp. Mol. Med.* **2013**, *45*, e53. [CrossRef] [PubMed]

16. Le, M.T.; Xie, H.; Zhou, B.; Chia, P.H.; Rizk, P.; Um, M.; Udolph, G.; Yang, H.; Lim, B.; Lodish, H.F. MicroRNA-125b promotes neuronal differentiation in human cells by repressing multiple targets. *Mol. Cell. Biol.* **2009**, *29*, 5290–5305. [CrossRef] [PubMed]

17. Frohlich, M.; Jaeger, A.; Weiss, D.G.; Kriehuber, R. Inhibition of BCL-2 leads to increased apoptosis and delayed neuronal differentiation in human ReNcell VM cells in vitro. *Int. J. Dev. Neurosci.* **2016**, *48*, 9–17. [CrossRef] [PubMed]

18. Mussmann, C.; Hubner, R.; Trilck, M.; Rolfs, A.; Frech, M.J. HES5 is a key mediator of Wnt-3a-induced neuronal differentiation. *Stem Cells Dev.* **2014**, *23*, 1328–1339. [CrossRef]

19. Williams, S.E.; Ratliff, L.A.; Postiglione, M.P.; Knoblich, J.A.; Fuchs, E. Par3-mInsc and $G\alpha_{i3}$ cooperate to promote oriented epidermal cell divisions through LGN. *Nat. Cell Biol.* **2014**, *16*, 758–769. [CrossRef]

20. Jia, M.; Li, J.; Zhu, J.; Wen, W.; Zhang, M.; Wang, W. Crystal structures of the scaffolding protein LGN reveal the general mechanism by which GoLoco binding motifs inhibit the release of GDP from $G\alpha_i$. *J. Biol. Chem.* **2012**, *287*, 36766–36776. [CrossRef]

21. Pan, Z.; Zhu, J.; Shang, Y.; Wei, Z.; Jia, M.; Xia, C.; Wen, W.; Wang, W.; Zhang, M. An autoinhibited conformation of LGN reveals a distinct interaction mode between GoLoco motifs and TPR motifs. *Structure* **2013**, *21*, 1007–1017. [CrossRef]

22. Baltoumas, F.A.; Theodoropoulou, M.C.; Hamodrakas, S.J. Interactions of the α-subunits of heterotrimeric G-proteins with GPCRs, effectors and RGS proteins: A critical review and analysis of interacting surfaces, conformational shifts, structural diversity and electrostatic potentials. *J. Struct. Biol.* **2013**, *182*, 209–218. [CrossRef]

23. McCaffrey, L.M.; Macara, I.G. Signaling pathways in cell polarity. *Cold Spring Harb. Perspect. Biol.* **2012**, *4*, a009654. [CrossRef]

24. Bergstralh, D.T.; Haack, T.; St Johnston, D. Epithelial polarity and spindle orientation: Intersecting pathways. *Philos. Trans. R. Soc. Lond. B Biol. Sci.* **2013**, *368*, 20130291. [CrossRef]

25. Lu, M.S.; Johnston, C.A. Molecular pathways regulating mitotic spindle orientation in animal cells. *Development* **2013**, *140*, 1843–1856. [CrossRef]

26. Sanada, K.; Tsai, L.H. G protein $\beta\gamma$ subunits and AGS3 control spindle orientation and asymmetric cell fate of cerebral cortical progenitors. *Cell* **2005**, *122*, 119–131. [CrossRef]

27. Morin, X.; Jaouen, F.; Durbec, P. Control of planar divisions by the G-protein regulator LGN maintains progenitors in the chick neuroepithelium. *Nat. Neurosci.* **2007**, *10*, 1440–1448. [CrossRef] [PubMed]

28. Blumer, J.B.; Chandler, L.J.; Lanier, S.M. Expression analysis and subcellular distribution of the two G-protein regulators AGS3 and LGN indicate distinct functionality. Localization of LGN to the midbody during cytokinesis. *J. Biol. Chem.* **2002**, *277*, 15897–15903. [CrossRef]

29. Fuja, T.J.; Schwartz, P.H.; Darcy, D.; Bryant, P.J. Asymmetric localization of LGN but not AGS3, two homologs of *Drosophila* Pins, in dividing human neural progenitor cells. *J. Neurosci. Res.* **2004**, *75*, 782–793. [CrossRef]

30. Ohata, H.; Miyazaki, M.; Otomo, R.; Matsushima-Hibiya, Y.; Otsubo, C.; Nagase, T.; Arakawa, H.; Yokota, J.; Nakagama, H.; Taya, Y.; et al. NuMA is required for the selective induction of p53 target genes. *Mol. Cell. Biol.* **2013**, *33*, 2447–2457. [CrossRef] [PubMed]

31. Choi, I.W.; Ahn, D.W.; Choi, J.K.; Cha, H.J.; Ock, M.S.; You, E.A.; Rhee, S.M.; Kim, K.C.; Choi, Y.H.; Song, K.S. Regulation of airway inflammation by G-protein regulatory motif peptides of AGS3 protein. *Sci. Rep.* **2016**, *6*, 27054. [CrossRef] [PubMed]

32. Wong, Y.H.; Conklin, B.R.; Bourne, H.R. G_z-mediated hormonoal inhibition of cyclic AMP accumulation. *Science* **1992**, *255*, 339–342. [CrossRef] [PubMed]

33. Kim, S.Y.; Ang, S.L.; Bloch, D.B.; Bloch, K.D.; Kawahara, Y.; Tolman, C.; Lee, R.; Seidmant, J.G.; Neer, E.J. Identification of cDNA encoding an additional a subunit of a human GTP-binding protein: Expression of three α_i subtypes in human tissues and cell lines. *Proc. Natl. Acad. Sci. USA* **1988**, *85*, 4153–4157. [CrossRef]

34. Strathmann, M.; Wilkie, T.M.; Simon, M.I. Diversity of the G-protein family: Sequences from five additional alpha subunits in the mouse. *Proc. Natl. Acad. Sci. USA* **1989**, *86*, 7407–7409. [CrossRef]

35. Ercolani, L.; Stow, J.L.; Boyle, J.F.; Holtzman, E.J.; Lin, H.; Grove, J.R.; Ausiello, D.A. Membrane localization of the pertussis toxin-sensitive G-protein subunits α_{i2} and α_{i3} and expression of a metallothionein-α_{i2} fusion gene in LLC-PKI cells. *Proc. Natl. Acad. Sci. USA* **1990**, *87*, 4637–4639. [CrossRef]

36. Gohla, A.; Klement, K.; Piekorz, R.P.; Pexa, K.; vom Dahl, S.; Spicher, K.; Dreval, V.; Haussinger, D.; Birnbaumer, L.; Nurnberg, B. An obligatory requirement for the heterotrimeric G protein G_{i3} in the antiautophagic action of insulin in the liver. *Proc. Natl. Acad. Sci. USA* **2007**, *104*, 3003–3008. [CrossRef]

37. Lou, X.; Mcquistan, T.; Orlando, R.A.; Farquhar, M.G. GAIP, GIPC and Gα$_{i3}$ are concentrated in endocytic compartments of proximal tubule cells: Putative role in regulating megalin's function. *J. Am. Soc. Nephrol.* **2002**, *13*, 918–927.

38. Nagata, K.; Okano, Y.; Nozawa, Y. Identification of heterotrimeric GTP-binding proteins in human megakaryoblastic leukemia cell line, MEG-01, and their alteration during cellular differentiation. *Life Sci.* **1995**, *57*, 1675–1681. [CrossRef]

39. Denis-Henriot, D.; de Mazancourt, P.; Goldsmith, P.K.; Giudicelli, Y. G proteins in adipocytes and preadipocytes: Characterization, subcellular distribution, and potential roles for G$_{i2}$ and/or G$_{i3}$ in the control of cell proliferation. *Cell Signal.* **1996**, *8*, 225–234. [CrossRef]

40. Ogier-Denis, E.; Houri, J.J.; Bauvy, C.; Codogno, P. Guanine nucleotide exchange on heterotrimeric G$_{i3}$ protein controls autophagic sequestration in HT-29 cells. *J. Biol. Chem.* **1996**, *271*, 28593–28600. [CrossRef] [PubMed]

41. Krumins, A.M.; Gilman, A.G. Targeted knockdown of G protein subunits selectively prevents receptor-mediated modulation of effectors and reveals complex changes in non-targeted signaling proteins. *J. Biol. Chem.* **2006**, *281*, 10250–10262. [CrossRef]

42. Oner, S.S.; Maher, E.M.; Gabay, M.; Tall, G.G.; Blumer, J.B.; Lanier, S.M. Regulation of the G-protein regulatory-Gα$_i$ signaling complex by nonreceptor guanine nucleotide exchange factors. *J. Biol. Chem.* **2013**, *288*, 3003–3015. [CrossRef]

43. Vural, A.; Fadillioglu, E.; Kelesoglu, F.; Ma, D.; Lanier, S.M. Role of G-proteins and phosphorylation in the distribution of AGS3 to cell puncta. *J. Cell Sci.* **2018**, *131*, jcs216507. [CrossRef]

44. Natochin, M.; Lester, B.; Peterson, Y.K.; Bernard, M.L.; Lanier, S.M.; Artemyev, N.O. AGS3 inhibits GDP dissociation from Gα subunits of the G$_i$ family and rhodopsin-dependent activation of transducin. *J. Biol. Chem.* **2000**, *275*, 40981–40985. [CrossRef] [PubMed]

45. Wong, Y.H.; Demoliou-Mason, C.D.; Barnard, E.A. ADP-ribosylation with pertussis toxin modulates the GTP-sensitive opioid ligand binding in digitonin-soluble extracts of rat brain membranes. *J. Neurochem.* **1988**, *51*, 114–121. [CrossRef]

46. Branham-O'Connor, M.; Robichaux, W.G., III; Zhang, X.K.; Cho, H.; Kehrl, J.H.; Lanier, S.M.; Blumer, J.B. Defective chemokine signal integration in leukocytes lacking activator of G protein signaling 3 (AGS3). *J. Biol. Chem.* **2014**, *289*, 10738–10747. [CrossRef]

47. Robichaux, W.G., III; Oner, S.S.; Lanier, S.M.; Blumer, J.B. Direct coupling of a seven-transmembrane-span receptor to a Gα$_i$ G-protein regulatory motif complex. *Mol. Pharmacol.* **2015**, *88*, 231–237. [CrossRef]

48. Conley, J.M.; Watts, V.J. Differential effects of AGS3 expression on D$_{2L}$ dopamine receptor-mediated adenylyl cyclase signaling. *Cell. Mol. Neurobiol.* **2013**, *33*, 551–558. [CrossRef]

49. Callihan, P.; Mumaw, J.; Machacek, D.W.; Stice, S.L.; Hooks, S.B. Regulation of stem cell pluripotency and differentiation by G protein coupled receptors. *Pharmacol. Ther.* **2011**, *129*, 290–306. [CrossRef]

50. Thomas, C.J.; Tall, G.G.; Adhikari, A.; Sprang, S.R. Ric-8A catalyzes guanine nucleotide exchange on Gα$_{i1}$ bound to the GPR/GoLoco exchange inhibitor AGS3. *J. Biol. Chem.* **2008**, *283*, 23150–23160. [CrossRef]

51. Tall, G.G. Ric-8 regulation of heterotrimeric G proteins. *J. Recept. Signal. Transduct. Res.* **2013**, *33*, 139–143. [CrossRef]

52. Tse, M.K.; Morris, C.J.; Zhang, M.; Wong, Y.H. Activator of G protein signaling 3 forms a complex with resistance to inhibitors of cholinesterase-8A without promoting nucleotide exchange on Gα$_{i3}$. *Mol. Cell. Biochem.* **2015**, *401*, 27–38. [CrossRef] [PubMed]

53. Chen, Q.; Kogan, J.H.; Gross, A.K.; Zhou, Y.; Walton, N.M.; Shin, R.; Heusner, C.L.; Miyake, S.; Tajinda, K.; Tamura, K.; et al. SREB2/GPR85, a schizophrenia risk factor, negatively regulates hippocampal adult neurogenesis and neurogenesis-dependent learning and memory. *Eur. J. Neurosci.* **2012**, *36*, 2597–2608. [CrossRef] [PubMed]

54. Kurabayashi, N.; Nguyen, M.D.; Sanada, K. The G protein-coupled receptor GPRC5B contributes to neurogenesis in the developing mouse neocortex. *Development* **2013**, *140*, 4335–4346. [CrossRef] [PubMed]

55. Yoshiura, S.; Ohta, N.; Matsuzaki, F. Tre1 GPCR signaling orients stem cell divisions in the *Drosophila* central nervous system. *Dev. Cell* **2012**, *22*, 79–91. [CrossRef]

56. Shinohara, H.; Udagawa, J.; Morishita, R.; Ueda, H.; Otani, H.; Semba, R.; Kato, K.; Asano, T. G$_{i2}$ signaling enhances proliferation of neural progenitor cells in the developing brain. *J. Biol. Chem.* **2004**, *279*, 41141–41148. [CrossRef]

57. Peng, H.; Huang, Y.; Rose, J.; Erichsen, D.; Herek, S.; Fujii, N.; Tamamura, H.; Zheng, J. Stromal cell-derived factor 1-mediated CXCR4 signaling in rat and human cortical neural progenitor cells. *J. Neurosci Res.* **2004**, *76*, 35–50. [CrossRef]

58. Tso, P.H.; Wang, Y.; Yung, L.Y.; Tong, Y.; Lee, M.M.; Wong, Y.H. RGS19 inhibits Ras signaling through Nm23H1/2-mediated phosphorylation of the kinase suppressor of Ras. *Cell Signal.* **2013**, *25*, 1064–1074. [CrossRef]

59. Lee, M.M.; Chui, R.K.; Tam, I.Y.; Lau, A.H.; Wong, Y.H. CCR1-mediated STAT3 tyrosine phosphorylation and CXCL8 expression in THP-1 macrophage-like cells involve pertussis toxin-insensitive $G\alpha_{14/16}$ signaling and IL-6 release. *J. Immunol.* **2012**, *189*, 5266–5276. [CrossRef]